3

GERRY-MEANDERING

Thus far we have examined several geometric measures of compactness as they relate to congressional districts. However, there is an additional geographic method of measuring whether or not congressional districts have been gerrymandered that we have not yet explored: meanderingness. Broadly speaking, meanderingness can be described in terms of being able to traverse a shape using straight lines. For example, polygons such as triangles and squares do not meander significantly, as a straight line can travel unimpeded between any two points in the shape. However, more complicated shapes are much harder to cross using straight lines, and thus we say that these shapes meander. (See Figure 1).

On a congressional level, certain districts have garnered attention over the years for how much they seem to meander throughout a state (See Figure 2). It seems apparent to the casual observer that such districts have been drawn with specific intent. Unfortunately, the appearance of gerrymandering is not enough to convince the Supreme Court that it has in fact taken place. Because of this, there has been a recent influx of mathematicians who have attempted to mathematically quantify meanderingness to lend credence to its potential judicial applications. In this chapter we will look at some of these attempts as well as the underlying geometry that makes it possible.

Figure 1: A shape that is very difficult to cross using straight lines [4]

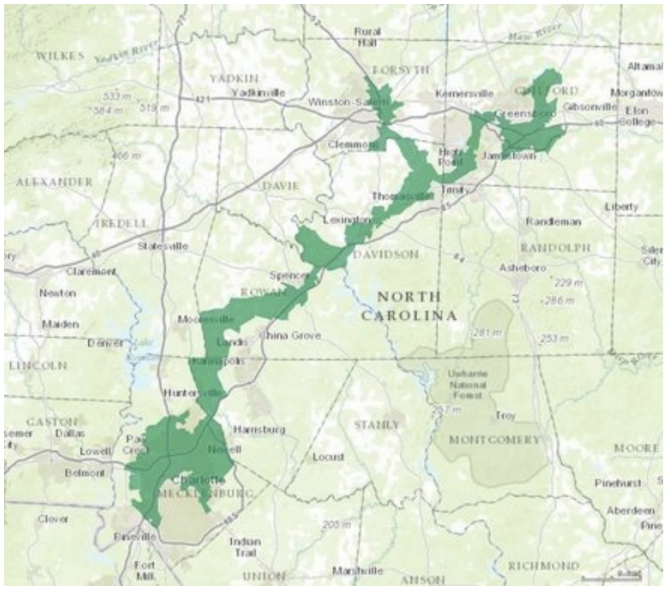

Figure 2: Former North Carolina District 12 [2]

3.1 HANDLEY'S MEANDERINGNESS TEST

Attempts to measure meanderingness– much like many of the other tests we have seen– arose after the Supreme Court communicated that they would be open to accepting mathematical measures of gerrymandering. In *Shaw v. Reno* (1993), the Court ruled that a citizen has the right under the Equal Protection Clause to challenge districts that were strangely shaped as potential racial gerrymanders [**Shaw**]. One of the first suggested approaches to measure meanderingness arose from *Johnson v. Miller*, a 1994 United States district court case in Georgia [**Johnson**]. In *Johnson v. Miller*, Georgia's eleventh congressional district was challenged, and Dr. Lisa Handley was called as an expert witness to propose a metric on how to classify a district as gerrymandered. Her measure is described in [2], and will be paraphrased here.

Dr. Handley's measure utilizes the fact that congressional districts are constructed using census blocks that are constructed by the United States Census Bureau. These blocks are small in area, sometimes only taking up a city block in urban areas. Prior to the 1990 census, only select portions of the country were divided into blocks. However, beginning in 1990 the Census Bureau began using census blocks for 100% of its tabulation [3]. This enabled Dr. Handley to develop the following method:

Consider a district D, and a census block B with central point P. Beginning at P, draw a line segment straight upward until it intersects a boundary of D. The ray may intersect multiple boundaries, but we will focus just on the intersection closest to P.

Label this point A_1. Repeat this process by shifting the line five degrees to the right, and label the new point of intersection A_2 ($\angle A_1PA_2$ should be five degrees). Repeat this process until you have a collection of 72 points around P. Draw closed line segments $\overline{A_1A_2}, \overline{A_2A_3}, \ldots, \overline{A_{71}A_{72}}, \overline{A_{72}A_1}$, forming a simple polygon. We call this polygon a *coverage polygon* of D, denoted $C(D)$. In theory, this coverage polygon approximates the portion of the congressional district that can be reached with straight lines emanating from P. Next, let $\alpha(D)$ equal the area of the district and $\alpha\big(C(D)\big)$ denote the area of the coverage polygon of D. Denote the total set of census blocks in this district $\mathcal{B}$. Repeat this process for every 25th census block in $\mathcal{B}$.

Definition 3.1.1. For any district D, the **meanderingness measure** of D is defined to be

$$\mu(D) = \max_{B \in \mathcal{B}} \left\{ \frac{\alpha\big(C(D)\big)}{\alpha(D)} \right\}$$

Example 3.1.2. What do high and low values of μ indicate about a district's meanderingness? What are the bounds of μ?

High and low values of μ are somewhat counter intuitive. A large value of μ indicates that the area of the largest coverage polygon is reasonably close to the area of the district, meaning that a majority of the district can be crossed with straight lines. This implies that the district does not meander significantly, and thus that it is not gerrymandered.

A low value of μ indicates that the district twists and turns enough that no census block can accurately be used to estimate its area using straight lines. This implies that the district meanders and was therefore gerrymandered.

As it is impossible for a district or coverage polygon to have negative area the meanderingness measure is bounded below by zero. However, μ technically has no upper bound. This is due to the fact that coverage polygons are constructed using 72 points, and thus districts have the potential to have razor thin divots or tendrils that are missed by the coverage polygon. However, given the nature of census blocks and the construction of congressional districts, the upper bound of μ is functionally 1.

At its core, this measure is attempting to mathematically quantify how much of a congressional district can be crossed using straight lines. Returning to Figure 2, by inspection we can see that any coverage polygon of this district would fail to cover a significant portion of its area, resulting in a low meanderingness measure. As we conjectured that this district was gerrymandered, a low meanderingness measure would support this claim.

Unfortunately, several problems with this measure quickly arise. Firstly, why only use every 25th census block? It seems as though a large amount of potentially crucial data is lost when only a fraction of census blocks are used. The answer lies in computing power. The 1990 census consisted of just over seven million census blocks, meaning that each of the 435 congressional districts comprised of an average of over 16,000 blocks each. Dr.

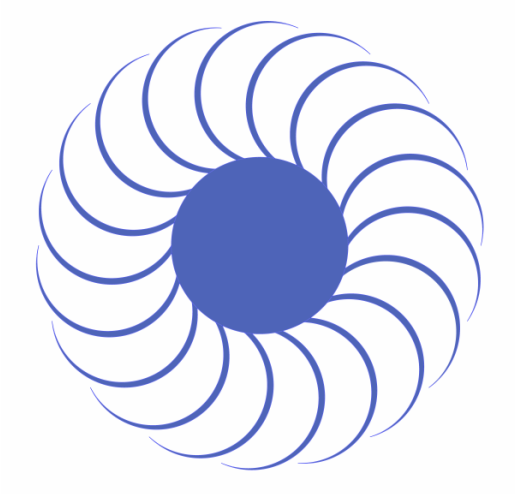

Figure 3: A hypothetical district with tendrils that could be missed by a coverage polygon. [2]

Handley contended that computing a coverage polygon for each individual census block would be highly unreasonable, especially given the computing power available in 1994. Indeed, from 1990 to 2010 the number of census blocks used has increased from seven to eleven million census blocks, bringing the average number per district up to roughly 25,000 [3].

The construction of these polygons using 72 points is also entirely arbitrary– any number of points could have been used. This choice was also made for computational purposes, but doing so opens the door to specific types of gerrymandering, as seen in Figure 3. Thankfully, technological power has drastically increased since the 1994 and thus it is now conceivable that coverage polygons could be computed for every census block. However, larger issues lie within the coverage polygons themselves.

The court was unconvinced by Dr. Handley's measure, citing the fact that a long, narrow, rectangular district that stretched for hundreds of miles would be considered as un-meandering and therefore not gerrymandered. Such a district would most certainly appear gerrymandered to the casual observer, revealing a fatal flaw of this meanderingness measure. Thus, we turn next to our main approach to measuring the meanderingness of a district: the medial-hull ratio.

3.2 VORONOI POLYGONS

In 2018, Eion Blanchard and Kevin Knudson proposed the medial-hull ratio as a new way to measure congressional district gerrymandering [2]. However, the medial-hull ratio is built on top of some pretty extensive geometry. Thus, some groundwork will need to be done before we can begin to discuss the medial-hull ratio's applications in gerrymandering - or even what it is. First, some basic definitions.

Definition 3.2.1. For any simple polygon, a vertex q is called **convex** if the internal angle at q is less than 180 degrees. Otherwise, the vertex is called **reflex**[1].

Definition 3.2.2. The **projection** of a point a onto the closed line segment $\overline{s_1, s_2}$ is the intersection of the line $\overleftrightarrow{s_1, s_2}$ and the line passing through a that intersects $\overleftrightarrow{s_1, s_2}$ perpendicularly.

Definition 3.2.3. A **convex set** S is a set of points such that, given any two points $x, y \in S$, the line joining them lies entirely within that set. Algebraically, a set S is convex if for all $x, y \in S$, $\lambda x + (1 - \lambda)y \in S$ for all $\lambda \in [0, 1]$.

Example 3.2.4. Show that a convex set cannot have a reflex internal angle.

Proof. Let S be a convex set. Suppose by way of contradiction that S has some reflex internal angle, $\angle abc$, for vertices $a, b, c \in S$. Consider the projection of b onto $\overline{ac}$. We will call this point p. Observe that because $\angle abc$ is a reflex angle $p \notin S$. However, as p is on a line joining two points in S, we have reached our contradiction, as this would prove that S is not convex. □

Theorem 3.2.5. *The intersection of any finite number of convex sets is convex.*

Proof. We will use induction. First, the base case: Let X and Y be convex sets, and let $z_1, z_2 \in X \cap Y$ and $z_3 \in \overline{z_1, z_2}$. As X is convex, $z_3 \in X$ because $z_3 \in \overline{z_1, z_2}$. As Y is convex, $z_3 \in Y$ because $z_3 \in \overline{z_1, z_2}$. Thus $z_3 \in X \cap Y$ and $X \cap Y$ is convex, verifying the base case.

Induction Step: Let $X_1, X_2, \ldots, X_n$ be convex sets. Suppose $X_1 \cap X_2 \cap \cdots \cap X_n$ is convex. Consider

$$X_1 \cap X_2 \cap \cdots \cap X_n \cap X_{n+1}$$

where X_{n+1} is convex. As $X_1 \cap X_2 \cap \cdots \cap X_n$ is a convex set, from the base case we know that the intersection of two convex sets is convex, and therefore

$$(X_1 \cap X_2 \cap \cdots \cap X_n \cap X_{n+1}) \cap X_{n+1}$$

is convex, completing the proof.

□

1 Technically a if a vertex has an internal vertex of exactly 180 degrees the vertex is a **flat** vertex. However, flat vertices will not be discussed here

Definition 3.2.6. A **hyperplane** is a convex set of the form $\{\vec{x} : \vec{a}^T\vec{x} = b\}$ for some vector $\vec{a}$ and some $b \in \mathbb{R}$.

Geometrically, hyplerplanes are subspaces that have a dimension that is one less than that of the space they inhabit. For example, hyperplanes in a three-dimensional space have two dimensions. Although they might seem a little out of the blue, hyperplanes will soon prove themselves essential.

Definition 3.2.7. The **bisector** $B(x, y)$ of two points x, y is the set of all points equidistant from x and y. The bisector $B(X, Y)$ of two sets of points X, Y is defined as

$$B(X, Y) = \{q : \min_{x \in X} d(q, x) = \min_{y \in Y} d(q, y)\},$$

with $d(a, b)$ denoting the Euclidean distance between a and b.

Lemma 3.2.8. *For any two distinct points in $\mathbb{R}^n$ the bisector is a hyperplane, and thus in $\mathbb{R}^2$ the bisector is a line.*

Proof. See [6]. Let $x = (x_1, \ldots, x_n)$ and $y = (y_1, \ldots, y_n)$ be two distinct points in $\mathbb{R}^n$. The bisector of x and y consists of the points $z = (z_1, \ldots, z_n)$ for which $d(x, z) = d(y, z)$. Squaring both sides yields $d(x, z)^2 = d(y, z)^2$, which can be written as

$$\sum_{i=1}^{n}(x_i - z_i)^2 = \sum_{i=1}^{n}(y_i - z_i)^2$$

These expressions can in turn be expanded to form

$$\sum_{i=1}^{n} x_i^2 - 2\sum_{i=1}^{n} x_i z_i + \sum_{i=1}^{n} z_i^2 = \sum_{i=1}^{n} y_i^2 - 2\sum_{i=1}^{n} y_i z_i + \sum_{i=1}^{n} z_i^2$$

These terms can be rearranged and combined to form

$$\sum_{i=1}^{n} x_i^2 - \sum_{i=1}^{n} y_i^2 = 2\sum_{i=1}^{n}(x_i - y_i)z_i,$$

which is equivalent to $||x||^2 - ||y||^2 = 2(x - y)^T z$, satisfying the equation of a hyperplane. As x, y are distinct, this completes the proof.

□

While some of these definitions and propositions might seem rather unrelated and sporadic, each will prove themselves absolutely necessary in the proofs to come. They also enable us to move on to the next major concept on our path to the medial-hull.

3.2.1 *Voronoi Regions*

Definition 3.2.9. Given a non-empty finite set S, we define the **Voronoi region** associated with a point $s \in S$ to be the set

$$V(s) = \{p : d(s,p) \leq d(s',p), \text{ for all } s' \neq s \in S\}$$

The Voronoi region of a point s is thus the set of all points in the plane that are closer to s than any other point in S. The simplest case for a Voronoi region is that in which S consists of a single point. In this instance the $V(s)$ would be equal to the entire space. For a set of two points, $S = \{s_1, s_2\}$, the Voronoi regions of these two points divide the plane into two half-planes divided by the perpendicular bisector of $\overline{s_1, s_2}$. Observe that these half-planes are not disjoint, and their intersection is the set of points that are equidistant from s_1 and s_2.

Lemma 3.2.10. *Let $P(x,y)$ denote the half-plane bounded by $B(x,y)$ that contains x. Then*

$$V(s) = \bigcap_{s \neq s'} P(s,s')$$

Proof. The following is a basic set equality proof.

- $\subseteq$ Let $x \in V(s)$. By definition, $d(s,x) \leq d(s',x)$ for all $s' \neq s \in S$. Thus, $x \in P(s,s')$ for every $s' \neq s \in S$. Thus, by definition of intersection, $x \in \bigcap_{s \neq s'} P(s,s')$.
- $\supseteq$ Let $x \in \bigcap_{s \neq s'} P(s,s')$. By definition of intersection, $x \in P(s,s')$ for every $s' \neq s \in S$. Thus $d(s,x_)) \leq d(s',x)$ for all $s' \neq s \in S$, with equality when x lies on the bisecting line. Thus, by definition of Voronoi polygon, Let $x \in V(s)$.

□

Corollary 3.2.11. *Let $s \in S$ with S non-empty and finite. Then $V(s)$ is non-empty and convex.*

Proof. See [7]. First we will show that $V(s)$ is convex. By Lemma 3.2.10 we know that $V(s)$ is the intersection of a finite number of half-planes. We know that these half-planes are formed using bisectors, which we know from Lemma 3.2.8 are hyperplanes and therefore convex. Thus, by Theorem 3.2.5, $V(s)$ is convex. As $V(s)$ is by definition associated with the point $s \in S$, we know that $s \in V(s)$ and therefore that $V(s)$ is non-empty. □

Theorem 3.2.12. *All points on the half-plane containing s_1 and not included in the perpendicular bisector l of $\overline{s_1 s_2}$ are closer to s_1 than s_2.*

Proof. See [8]. Let p be a point such that p lies in the half-plane containing s_1. Let b be the projection of p onto $\overline{s_1, s_2}$, and let m denote the midpoint between s_1 and s_2. Consider the right triangles $\triangle\, s_1 pb$ and $\triangle\, s_2 pb$ (See Figure 4). These triangles share the side $\overline{pb}$.

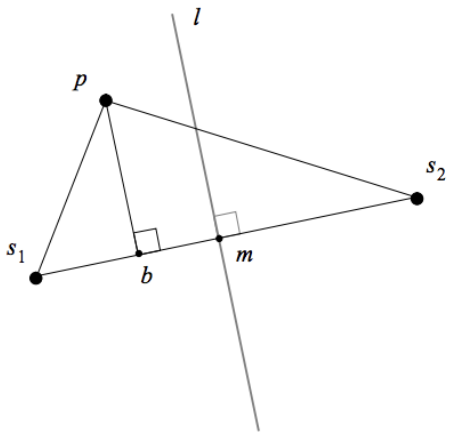

Figure 4: A visualization of Theorem 3.2.12 [8]

As $d(s_1, m) = d(s_1, b) + d(b, m)$ and $d(s_1, m) = d(s_2, m)$ we see that $\overline{s_1 b}$ is shorter than $\overline{bs_2}$. Thus, by the Pythagorean theorem we see that the hypotenuse of $\triangle\, s_1 pb$, $\overline{s_1 p}$ is shorter than the hypotenuse of $\triangle\, s_2 pb$, $\overline{s_1 p}$. Thus, p is closer to s_1 than s_2.

□

Theorem 3.2.13. *Assume that s_1, s_2, and s_3 are not co-linear. The intersection of the 3 perpendicular bisectors of s_1, s_2 and s_3 is the center of the circle containing s_1, s_2 and s_3.*

Proof. See [8]. As s_1, s_2, and s_3 are not co-linear, we know that the intersection exists. Let s_1, s_2, and s_3 be points with three perpendicular bisectors that intersect at a point c. Let b be the midpoint of $\overline{s_1 s_2}$. Construct two triangles $\triangle\, s_1 bc$ and $\triangle\, s_2 bc$. The perpendicular bisector of s_1 and s_2 is equidistant from those two points, and thus $\overline{s_1 b}$ and $\overline{s_2 b}$ are equal in length. As the bisector is perpendicular, the angles $\angle s_1 bc$ and $\angle s_2 bc$ are right angles. Note that because both triangles share the side $\overline{bc}$ they must be congruent, meaning their hypotenuses, r_1 and r_2, are equal. This argument holds for the s_1, s_3 and s_2, s_3 triangles as well. Thus we have shown that the point c is equidistant from s_1, s_2, and s_3, and is therefore the center of the circle containing s_1, s_2 and s_3 (See Figure 5). □

Thus far we have worked with isolated elements of our sets, whether they be points in the plane or edges of a polygon. However, it is possible to combine these Voronoi regions into something more cohesive.

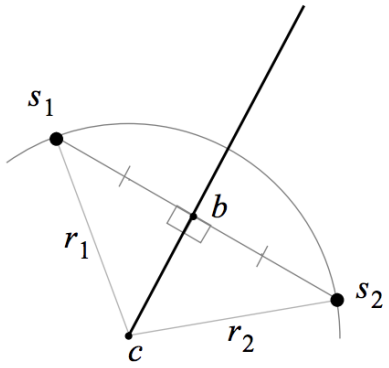

Figure 5: A visualization of Theorem 3.2.13 [8]

Definition 3.2.14. The collection of Voronoi regions for each element of S is called the **Voronoi diagram** of the set S and is denoted $V(S)$.

$$V(S) = \bigcup_{s \in S} V(s)$$

Voronoi regions effectively partition a space into regions based on proximity to points in S. Recall, however, that not all Voronoi regions are disjoint, as some points are equidistant from two points in S. Thus Voronoi diagrams do not technically partition the set S because there exist elements that fit into more than one subset– these intersections form the edges of the Voronoi diagram. Even though the Voronoi diagream does not fulfill the definition of a partition, it does come very close; the subset of the space that specifically excludes these equidistant points would in fact be partitioned by the Voronoi diagram.

There is a special case that must be addressed before we can continue. Consider a set of n points S in which all points in S are co-linear. The Voronoi diagram of this set would be a series of $n - 1$ parallel lines, each of them a perpendicular bisector of a line segment adjoining two adjacent points. If this case is discarded, some interesting properties can be observed.

Theorem 3.2.15. *Let S be a set that in which all points are not co-linear. For each vertex v of $V(S)$, the following statements hold:*

(1) v is the intersection of at least three edges of $V(S)$

(2) There exist at least three points $s_1, s_2, s_3 \in S$ such that v is incident to $V(s_1), V(s_2)$, and $V(s_3)$.

(3) v is the center of a circle $C(v)$ through at least three points of S such that $C(v) \cap S = \emptyset$

Proof. See [7].

(1) Let v be a vertex of $V(S)$. By Corollary 3.2.11 each Voronoi diagram is convex. If v were incident to less than three edges of $V(S)$ that would mean that one of the diagrams would have to have a reflex angle, which would contradict Example 3.2.4. Thus, v is the intersection of at least three edges of $V(S)$.

(2) By (1) we know that v is at the intersection of at least three edges of $V(S)$. Thus there exist at least three regions, $V(a), V(b), V(c)$, such that v is at their intersection. Thus it follows that there exist at least three points, a, b, c, such that v is incident to $V(s_1), V(s_2)$, and $V(s_3)$.

(3) The edge of a Voronoi diagram between Voronoi regions $V(s)$ and $V(t)$ is the perpendicular bisector of $\overline{st}$. By (2) we know then that v is the intersection of at least three perpendicular bisectors of a, b, and c. Thus, by Theorem 3.2.13, v is the center of a circle, which we will denote $C(v)$, through at least three points of S.

Next, suppose by way of contradiction that there exists some point x such that $x \in C(v) \cap S$. Then v would be closer to x than any other point in S, which contradicts the fact that v is in at least $V(a), V(b)$, and $V(c)$. [8]

□

The following corollary was stated in [7] and will will be proved below.

Corollary 3.2.16. *Let S be a set that in which all points are not co-linear. Assume that no four points in S are co-circular. For each vertex v of $V(S)$, the following statements hold:*

(1) v is the intersection of exactly three edges of $V(S)$

(2) There exists points $s_1, s_2, s_3 \in S$ such that v is incident to $V(s_1), V(s_2)$, and $V(s_3)$.

(3) v is the center of a circle $C(v)$ through exactly three points of S such that $C(v) \cap S = \emptyset$

Proof. Suppose by way of contradiction that there exist n edges of $V(S)$ where $n > 3$. Following an analogous argument to that made in Theorem 3.2.15 we can see that v is the center of a circle $C(v)$ through all n points. This contradicts our assumption that no four points in S are co-circular. The same argument can be made for parts (2) and (3), completing the proof.

□

3.2.2 *Voronoi Polygons*

It is possible to construct Voronoi regions for shapes as well as sets of points, as seen in the following definition. Doing so will take us one massive step closer to being able to apply these regions to the political sphere.

Definition 3.2.17. Consider a simple polygon G with a vertex set V and edge set E. Using the interior of G as our space we can construct a **Voronoi polygon** of each edge $e_i = \overline{v_i, v_{i+1}} \in E$, $V(e_i)$, using E as our set S. Instead of each element being a point, however, we use edges of the polygon. In other words, we say that a point $p \in V(e_i)$ if

$$\min\{d(x,p) : x \in e_i\} \leq \min\{d(y,p) : y \in e_j\}$$

for some $p \in G$ and edges $e_i \neq e_j \in E$.

Constructing Voronoi regions for the entire boundary of a simple polygon G in this way would 'partition' the interior of G into subsets depending on which edge of the polygon a point is closest to. Unfortunately it is not always the case that the Voronoi diagram of G is equal to the union of the Voronoi regions associated with the edges of G. This is due to the existence of the case where G has a reflex vertex. Reflex vertices technically belong to two edges of the polygon, but the following theorem highlights an issue that would arise were they not distinguished separately.

Theorem 3.2.18. *Let G be a simple polygon with boundary B and interior I with a reflex vertex v_i. There exists a non-empty set*

$$V^*(v_i) = \{x \in I : d(v_i, x) < d(z, x) \text{ for all } z \in B\}$$

Note here that the inequality in $V^*(v_i)$ is strict, whereas $V(v_i)$ would also include any points that are equidistant from v_i and some other boundary point, should it exist.

Proof. Let G be a simple polygon with boundary B and interior I with a reflex vertex v_i. Consider the set

$$V^*(v_i) = \{x \in I : d(v_i, x) < d(z, x) \text{ for all } z \in B\}.$$

As v_i is a vertex of a simple polygon there exist two adjacent vertices, v_{i-1} and v_{i+1}. Without loss of generality we will say that v_{i-1} is to the left of v_i and v_{i+1} is to the right. Consider the line B bisecting the angle $\angle v_{i-1}v_iv_{i+1}$ and the perpendicular line P that intersects this bisecting line at v_i. As e_{i-1} and e_i are edges and therefore sets of points we can invoke the definition of the bisector of two sets to see that B is the set of all points which are equidistant to some boundary point of both e_{i-1} and e_i. Thus we say that all of the points of P that are to the left of v_i, denoted $P_\ell \subset P$, are closer e_{i-1} and all of the points that are to the right of v_i are closer e_i, denoted $P_r \subset P$.

For each $a \in P_\ell$ such that $a \in I$, let a' denote the projection of a onto e_{i-1}. Equivalently, for each $a \in P_r$ such that $a \in I$, let a' denote the projection of a onto e_i. Note that because v_i is reflex $a \neq a'$ and thus $d(a, a') \geq 0$ for all $a \in P$. Additionally, notice that we are using a to denote points on either side of v_i.

Let z be the closest boundary point to v_i that is not in either e_{i-1} or e_i. Consider the circle of radius $\frac{d(v_i,z)}{2}$ centered at v_i, denoted $C(v_i)$. Let x be a point such that $x \in C(v_i) \cap B$.

For all $a \neq v_i \in P$, the triangle $\triangle\, xv_ia$ will be a right triangle with hypotenuse $\overline{xa}$. Thus by the Pythagorean theorem, v_i is closer to x than any other point of P. As $d(a, a') \geq 0$ for all $a \in P$, we can also say that v_i is closer to x than any other points of e_{i-1} and e_i. Finally, as we defined our circle such that no other boundary point of G is touched, we have shown that there exists a point x such that $d(v_i, x) < d(z, x)$ for all $z \in B$. Thus $x \in V(v_i)$, completing the proof.

□

When constructing Voronoi diagrams for non-convex polygons we could use the same formula as the one given in Definition 3.2.14, but Theorem 3.2.18 shows us that there exists a subset of G that is closer to the reflex vertex than any other boundary point of the polygon. As reflex vertices are the intersection of two edges, this definition would result in the Voronoi regions of those two edges overlapping for the entire set $V^*(v_i)$. This does not even come close to partitioning G, and thus we will modify our definition.

Definition 3.2.19. Let G be a simple polygon. Let $V = \{v_1, v_2, \ldots, v_n\}$ be the vertex set of G, $R\{v_{r_1}, v_{r_2}, \ldots, v_{r_m}\} \subset V$ be the set of all reflex vertices of G, and $E = \{e_1, e_2, \ldots, e_{n-1}\}$ be the set of edges of G. Then

$$V(G) = \bigcup_{i=1}^{n-1} V(e_i - R) \cup \bigcup_{j=1}^{m} V(v_{r_j})$$

This definition fixes our earlier conundrum by giving each reflex vertex of G its own Voronoi region, removing the issue of regions overlapping.

Example 3.2.20. Let G be a convex polygon with a vertex set $V = \{v_1, v_2, \ldots, v_n\}$ and edge set $E = \{e_1, e_2, \ldots, e_{n-1}\}$. Then

$$V(G) = \bigcup_{i=1}^{n-1} V(e_i)$$

Proof. This proof follows from the definition of unions of sets and the fact that if e_i has no reflex vertices then $e_i - R = e_i$. □

Now that can construct Voronoi diagrams of simple polygons we have finally assembled all of the tools we need to dive into the medial-hull ratio. We begin by focusing on the 'medial' portion of 'medial-hull'.

3.3 THE MEDIAL AXIS

Definition 3.3.1. Let G be an arbitrary simple polygon with boundary B and interior I. The **medial axis** of G, denoted $\mathcal{M}(G)$, is the set of points in the interior of G which have more than one closest point on the boundary of G.

$$\mathcal{M}(G) = \{p \in I : d(x, p) = d(y, p) \leq d(z, p) \text{ for all distinct } x, y, z \in B\}$$

The medial-axis cen equivalently be described as the set of the centers of maximal circles contained in G.

Example 3.3.2. By hand, attempt to draw medial axes for a square, circle, triangle, and rectagle. If you are feeling adventurous, attempt to draw the medial axes of a block letter E.

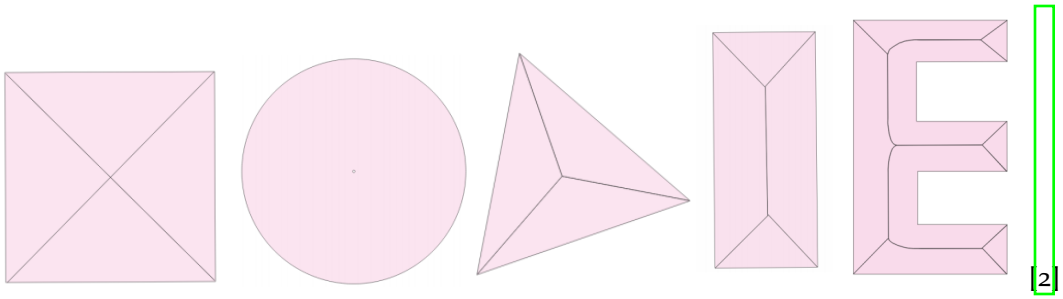

[2]

The following proposition was stated in [5], and will will be proved below.

Lemma 3.3.3. *Let G be a simple polygon. For edges of G, e_i and e_j, the Voronoi polygons $V(e_i)$ and $V(e_j)$ share an edge if and only if there exists a point z such that the circle centered at z with radius $d(z, e_i) = d(z, e_j)$ does not include any boundary point of G in its interior.*

Proof. Recall the definition of Voronoi polygons associated with edges of planar shapes.

($\Rightarrow$) Let e_i and e_j be elements such that $V(e_i)$ and $V(e_j)$ share an edge. Thus $V(e_i) \cap V(e_j) \neq \emptyset$ and there exists some point z such that $z \in V(e_i) \cap V(e_j)$. From the definition of Voronoi polygons it follows that

$$d(e_i, z) \leq d(e_j, z) \quad \text{and} \quad d(e_j, z) \leq d(e_i, z),$$

implying that $d(e_i, z) = d(e_j, z)$. Consider the circle of radius $d(e_i, z) = d(e_j, z)$ centered at z, $C(z)$. Suppose by way of contradiction there exists some boundary point p of G such that p lies in the interior of $C(z)$. As p is on the boundary of G, there exists some $k \neq i, j$ such that $1 \leq k \leq n-1$ and $p \in e_k$. As p lies in the interior of $C(z)$, z is closer to e_k than e_i and e_j, and thus

$$d(e_k, z) \leq d(e_i, z) = d(e_j, z),$$

which would imply that $z \notin V(e_i) \cap V(e_j)$, a contradiction. Therefore $C(z)$ cannot contain any boundary point of G in its interior.

($\Leftarrow$) Suppose there exists a point z such that the circle centered at z with radius $d(z, e_i) = d(z, e_j)$ does not include any boundary point of G in its interior. As there is no boundary point of G in the interior of the circle, $d(z, e_i) = d(z, e_j) \leq d(z, e_k)$ for all $k \neq i, j$ such that $1 \leq k \leq n-1$. Thus $z \in V(e_i)$ and $z \in V(e_j)$, implying that $z \in V(e_i) \cap V(e_j)$. By Lemma 3.2.10, $z \in P(e_i, e_j)$ and $z \in P(e_j, e_i)$. Therefore z must lie on the boundary between $V(e_i)$ and $V(e_j)$. It follows that they must share an edge.

□

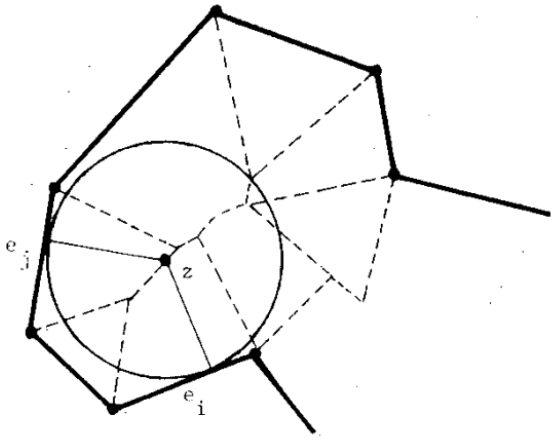

Figure 6: A visualization of Lemma 3.3.3 [5]

Corollary 3.3.4. *Let G be a simple polygon. For an edge of G, e_i, with a reflex endpoint, v_i, the Voronoi polygons $V(e_i)$ and $V(v_i)$ share an edge (See Figures 7 and 8).*

Proof. By Theorem 3.2.18, we know there exists a point z that is closer to v_i than any other boundary point of G. As $v_i \in e_i$, the circle centered at z with radius $d(z, e_i) = d(z, v_i)$ does not include any boundary point of G in its interior. Thus, by Lemma 3.3.3 $V(e_i)$ and $V(v_i)$ share an edge. □

Observe that while this lemma refers specifically to edges of G, an analogous argument shows the same result for edges of G *and* reflex vertices of G. The difference lies in the fact that Lemma 3.3.3 does not specify that these edges be distinct.

The following theorem was stated in [5] and ties everything together. It will be proven below.

Theorem 3.3.5. *Let G be a simple polygon with boundary B. The medial axis of G is the set of Voronoi edges of G without the edges incident with reflex vertices, denoted $V'(G)$.*

Proof. The following is a slightly less basic set equality proof.

($\subseteq$) Let $p \in \mathcal{M}(G)$. Thus there exist distinct $x, y \in B$ such that for all $z \in B$:

$$d(x, p) = d(y, p) \leq d(z, p).$$

This means that there exist at least two points on the boundary of G such that p is equidistant. As $x, y \in B$, there exist edges e_i, e_j such that $x \in e_i$ and $y \in e_j$. Consider the circle of radius $d(p, x) = d(p, y)$ centered at p. As this circle does not include any boundary point of G in its interior, by Lemma 3.3.3 p is on an edge shared by $V(e_i)$ and $V(e_j)$.

The definition of medial axis specifies x and y must be distinct. However, if x was a reflex vertex, by Theorem 3.2.18 $d(x,p) < d(z,p)$ for all $z \in B$. Therefore the only case in which the circle of radius $d(p,x) = d(p,y)$ centered at p exists is when $x = y$. Thus, when the Voronoi edge is incident to a reflex vertex, none of the points on that particular edge are in the medial axis. It follows that if $p \in \mathcal{M}(G)$, it must be the case that $p \in V'(G)$.

($\supseteq$) Let $p \in V'(G)$. Then there must exist Voronoi edges e_i and e_j such that

$$d(e_i, p) = d(e_j, p) \leq d(z, p).$$

Recall that $V'(G)$ does not contain any of the edges of $V(G)$ that are incident to reflex vertices, and are therefore closer to the reflex vertex than any other boundary point of G. Thus we can assume that $e_i \neq e_j$. It follows that there exist at least two points on the boundary of G such that p is equidistant. From this we can conclude that $p \in \mathcal{M}(G)$.

□

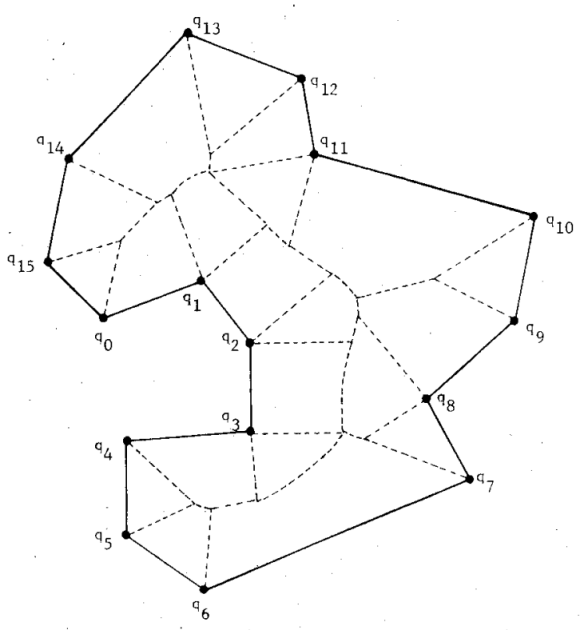

Figure 7: Voronoi diagram of a simple polygon [5]

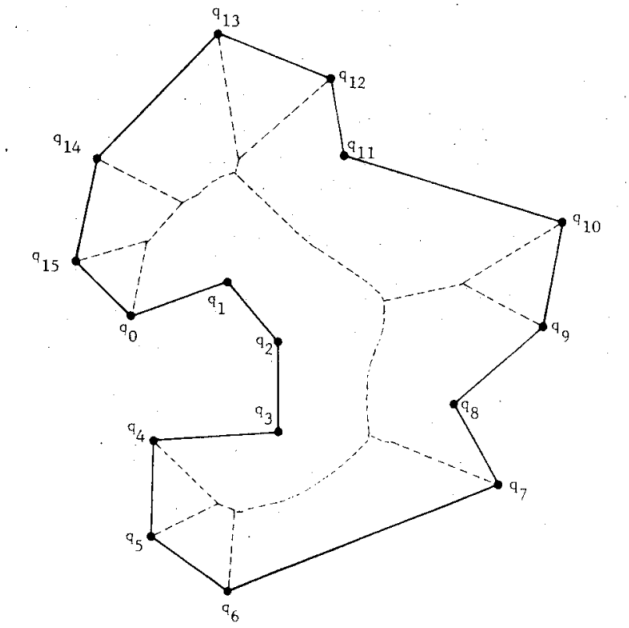

Figure 8: Medial axis of a simple polygon [5]

3.3.1 *The Medial-Hull Ratio*

We've done it! Through perseverance and sheer force of will we have unlocked the secrets necessary to assemble the medial-hull ratio, our next and final measure of congressional district meandering. As you may have surmised, the 'hull' portion of the medial-hull ratio refers to the convex hull of a polygon, which you may remember from the sections on compactness.

Definition 3.3.6. Let $\mathcal{M}(P)$ denote the medial axis of a polygon P and let $\mathcal{C}(P)$ denote the clipped convex hull of P[2]. Finally, let $|A|$ denote the length of an axis A. We define the **medial-hull ratio** of a polygon P as

$$\mathcal{R}_P = \frac{|\mathcal{M}(P)|}{|\mathcal{M}(\mathcal{C}(P))|}$$

The remainder of this section is explored in [2], in which Blanchard and Knudson describe and apply the medial-hull ratio, as well as establish a four tier categorization for medial-hull ratios will be included here as well.

2 Clipping the convex hull essentially means that it will not include any area not contained within the state (such as coasts, other states, etc)

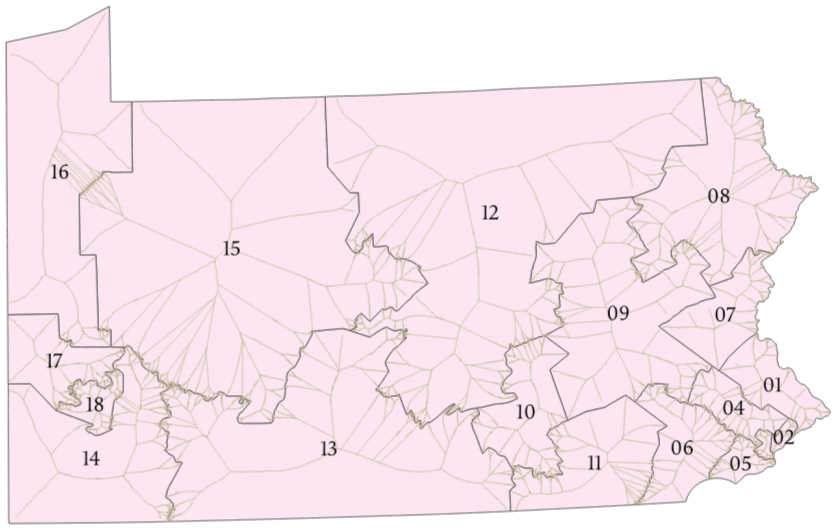

Figure 9: Medial Axes of Pennsylvania congressional districts [2]

A district D is placed in Category 1 if $\mathcal{R}_D < 2.00$. Districts in Category 1 exhibit no explicit evidence of gerrymandering under this method of analysis. D is placed in Category 2 if $2.00 \leq \mathcal{R}_D < 2.40$. Districts in Category 2 bear some evidence of gerrymandering. Districts in Category 3, which includes districts with $2.40 \leq \mathcal{R}_D < 2.80$, have enough evidence to suggest that the district was probably gerrymandered. Districts with $2.80 \leq \mathcal{R}_D$ are placed in Category 4, which implies that the district was almost certainly gerrymandered.

3.3.2 *District Computation*

With this categorization in place, Blanchard and Knudson were able to calculate medial-hull ratios for a variety of congressional districts. In total, they computed ratios for 335 districts from 22 states. In Figure 9, we see the medial axes for each of Pennsylvania's 18 congressional districts. Figure 10 details the medial-hull ratios for each of these districts.

Pennsylvania District 12 garnered the highest score with 3.22, placing it steadfastly in Category 4. However, District 12 is the only Category 4 district.[3] Four districts would be placed in Category 3, indicating probable evidence of gerrymandering. However, over half of Pennsylvania's districts would be placed into Category 1, indicating little to no

3 Although the table presents District 13 as having a medial-hull ratio of 2.80, it is actually 2.79916, and would thus technically reside in Category 3.

district	medial axis (km)	hull axis (km)	medial-hull ratio
1	272.307	219.004	1.24
2	56.499	48.785	1.16
3	50.614	48.314	1.05
4	293.153	114.151	2.57
5	154.501	97.631	1.58
6	485.474	209.564	2.32
7	309.882	269.618	1.15
8	1,066.613	860.578	1.24
9	1,013.247	458.032	2.21
10	450.228	221.009	2.04
11	575.273	230.564	2.50
12	1,770.610	550.574	3.22
13	1,341.484	479.245	2.80
14	659.797	336.675	1.96
15	1,983.138	739.098	2.68
16	671.614	342.713	1.96
17	330.171	188.000	1.76
18	234.392	119.128	1.97

Figure 10: Medial-Hull data for Pennsylvania districts [2]

evidence of gerrymandering. In fact, Pennsylvania's medial-hull average would be placed in Category 1.

Figure 11 details average medial-hull ratios for all 22 states from which districts were sampled. One may notice an immediate discrepancy between the previous two figures. This is because Pennsylvania's original district drawing was ruled unconstitutional, and a remedial map was drawn. This the map seen above, with an average medial-hull ratio in Category 1. The unconstitutional drawing would have been placed into Category 3. It should also be stated that the medial-hull average for districts in Washington state was 2.01 except for two outliers, which drastically increased the average. These outliers were not exceptionally gerrymandered, however, and instead fell victim to some of the issues we will discuss in the next section.

3.3.3 *Issues with the Medial-Hull Ratio*

The medial-hull ratio is not without its faults. There exist several issues with the ratio have been identified thus far. A few of these pertain specifically to the program written by [2] to compute medial-hull ratios for congressional districts. As these weaknesses are computational in nature they will not be discussed at great length.

The first issue that arises is that of combs. These are computing errors that occurred in the computation of the medial axis that carried through to the final product. These errors,

state	districts	avg. medial-hull ratio
Washington	10	2.51
Pennsylvania	18	2.50
Arkansas	4	2.37
North Carolina	13	2.32
Virginia	11	2.30
California	53	2.20
Texas	36	2.20
Louisiana	6	2.14
Ohio	16	2.08
Arizona	9	2.04
Georgia	14	2.02
Pennsylvania (remedial)	18	1.97
Maryland	8	1.96
Illinois	18	1.79
New Jersey	12	1.71
Florida	27	1.65
Oklahoma	5	1.60
Michigan	14	1.53
Indiana	9	1.52
New York	27	1.50
Nevada	4	1.26
West Virginia	3	1.21

Figure 11: Medial-Hull averages for several US states [2]

which resemble combs in appearance, were most likely attributed to the software used and how it treated specific Voronoi polygons. In response, [2] suggests that adding distant vertices before creating the Voronoi region in an attempt to push the combs outside the boundary of the district.

Infinite fragments have also been known to pop up in certain districts. These are errors in which sections of the medial axis which have reasonably small geographic area are measured to have near infinite length. Although a manual removal of the region can be performed via trial and error, no solutions to this issue has been proposed thus far.

The next point of concern calls back to the issues with compactness measures discussed in the previous chapter. Intuitively, the medial axis of the convex hull should be simpler and thus shorter than its congressional counterpart. However, there exist instances when this is not the case. The medial-hull ratio is susceptible to coastline effects, which can have un-intuitive impacts on the ratio. Consider the case in which a district lies on a jagged coastline. This will result in the medial axis having many skeletal limbs stretching out to these jagged edges, as would be expected. However, as these edges are from the state's border, the clipped convex hull will not smooth over these edges, and the limbs of the medial axis will remain. Yet, the opposite side of the district may be concave, and in this case the medial-hull will smooth over these areas. This will pull the central spine of the medial axis away from the jagged edges, increasing its overall length. Thus it is

possible to have a congressional district with a medial-hull ratio less than one. A possible solution to this would be to smooth over such coastlines. This would avoid penalizing jagged district boundaries which are caused by state borders.

There are circumstances in which a district may share a border with a squarish, compact district, but also have a separate edge that is highly jagged and looks gerrymandered to the eye. However, the border with the squarish district may to some degree counteract the jagged portion, lessening the ratio as a whole. Thus it is possible for districts that are partially gerrymandered in this way to slip under the radar.

If a congressional district is itself convex, then it will be equal to its convex hull, resulting in a medial-hull ratio of 1.00. This would also be the case when a district is almost convex except for a jagged state border. It is possible to create gerrymandered districts that are still compact; these districts would not be detected by the medial-hull measure.

Unfortunately, this error is a judicially fatal one. Recall the example of an extremely long rectangular district proposed in *Johnson v Miller*. This district would have been viewed as compact for Dr. Handley's meanderingness measure, and was thus enough grounds for the court to cast aside her argument. As rectangles are convex polygons, this district would also be seen as compact and 'fair' under the medial-hull ratio. No solutions to this conundrum have been posed, and thus the potential judicial applications of the medial-hull ratio seem slim to none.

That being said, progress is not linear. Neither is success. Measuring meanderingness may not look viable today, but that does not mean that it will not be viable tomorrow. Breakthroughs have occurred in mathematics in even the most desolate of places, and there could come a day sometime soon when meanderingness proves its worth on the judicial stage. More importantly, meanderingness measures such as these show that progress is being made. In the last decade the mathematical community has seen a surge in attempts to quantify and identify congressional gerrymandering. No stone is being left un-turned. Even if meanderingness is not the solution, it may inspire others to look in new directions and search for new ideas. But the inspiration does not stop here. In the next chapter we will move beyond compactness into new fields of discovery- focusing not on the geography of the districts but the voters that inhabit them.

REFERENCES

[1] Franz Aurenhammer and Rolf Klein. "Voronoi diagrams". In: *Handbook of computational geometry* 5.10 (2000), pp. 201–290.

[2] Eion Blanchard and Kevin Knudson. "Measuring Congressional District Meandering". In: *arXiv preprint arXiv:1805.08208* (2018).

[3] US Census Bureau. *What are census blocks?* 2011. URL: https://www.census.gov/newsroom/blogs/random-samplings/2011/07/what-are-census-blocks.html.

[4] hddfhm. *Silhouette cowboy clipart*.

[5] Der-Tsai Lee. "Medial axis transformation of a planar shape". In: *IEEE Transactions on Pattern Analysis & Machine Intelligence* 4 (1982), pp. 363–369.

[6] University of Saint Andrews. *Homework 2 Solutions*. 2004. URL: http://www-groups.mcs.st-and.ac.uk/~vince/teaching/summer04/354hw2soln.pdf.

[7] Semantischolor.org. *Chapter 7: Voronoi Diagrams*. 2017. URL: https://pdfs.semanticscholar.org/ac13/4ee505d074de5f86c379452bca2aedd88737.pdf.

[8] Roberto Tamassia. *Introduction to Voronoi Diagrams*. 1992. URL: http://cs.brown.edu/courses/cs252/misc/resources/lectures/pdf/notes09.pdf.